

PACS numbers: 42.30.Wb; 42.25.Fx; 05.10.Ln
DOI: 10.1070/QE2005v035n02ABEH003337

Monte Carlo simulation of an optical coherence Doppler tomograph signal: the effect of the concentration of particles in a flow on the reconstructed velocity profile

A.V. Bykov, M.Yu. Kirillin, A.V. Priezzhev

***Abstract*. Model signals of an optical coherence Doppler tomograph (OCDT) are obtained by the Monte Carlo method from a flow of a light-scattering suspension of lipid vesicles (intralipid) at concentrations from 0.7 % to 1.5 % with an *a priori* specified parabolic velocity profile. The velocity profile parameters reconstructed from the OCDT signal and scattering orders of the photons contributing to the signal are studied as functions of the suspension concentration. It is shown that the maximum of the reconstructed velocity profile at high concentrations shifts with respect to the symmetry axis of the flow and its value decreases due to a greater contribution from multiply scattered photons.**

Keywords: *Monte Carlo method, light scattering, optical coherence Doppler tomography, coherence length, velocity profile, intralipid.*

1. Introduction

Optical coherence Doppler tomography (OCDT) [1 – 3] is a modern noninvasive optical method for measuring flow velocities in highly scattering media. The possible applications of this method are the measurement of the bloodflow velocity in near-surface layers of tissues *in vivo* with the simultaneous visualisation of velocity profiles of different complexity and the solution of various rheological problems of studying the flow of scattering liquids through capillaries with a complex geometry [4]. An optical coherence Doppler tomograph is based on a Michelson interferometer with one of the arms containing a scanning reference mirror and another one – a living object or a continuous-flow vessel with the liquid under study. OCDT based on the principles of low-coherence interferometry uses mainly singly or low-order scattered photons of all the photons backscattered from the object under study consisting of moving and immobile scatters. This is achieved by employing broadband light sources, for example, femtosecond lasers or superluminescent diodes (SLDs) and by forming a desired signal only by light scattered from a small measurement region. The longitudinal size of this region is determined by the coherence length of the probe beam (about 15 μm for a SLD), while the transverse size – by the numerical aperture of a focusing lens. Photons scattered by moving particles make a contribution to the signal with a certain Doppler frequency shift, which linearly depends on the velocity of scattering particles. Scanning over the flow depth performed by moving the reference mirror gives the spatial distribution (profile) of the velocity of moving particles.

However, the contribution from multiple scattered photons to the output OCDT signal cannot be completely eliminated in experimental setups. The number of such photons depends on the concentration of scatterers in the liquid flow under study. Because of a random nature of their trajectories, these photons have random Doppler frequency shifts, resulting in the distortion of the reconstructed velocity profile compared to the real one. To develop the methods for eliminating or minimising the velocity profile distortions, it is necessary to study the distribution of photons contributing to the OCDT signal over the scattering order as a function of the concentration of scatterers in the liquid flow and to estimate the extent of their influence on the reconstructed velocity profile.

The Monte Carlo simulation is a convenient tool for studying the propagation of light in highly scattering media and the signal formation in various experimental setups, including OCDT [5 – 9]. In particular, this method was used [9] to study the influence of the scattering order of photons contributing to the OCDT signal on its attenuation by considering separately contributions of low-order and multiple scattering.

The contributions of different scattering orders to the backscattered light intensity were already discussed in our previous papers [10, 11]. In particular, we showed that scattering of light from a layer of the erythrocyte suspension to the forward half-plane is mainly determined by photons weakly changing the direction of their propagation in a medium (snake photons), whereas the intensity of scattering to the back half-plane is characterised by more uniform angular and scattering-order distributions. The aim of this paper is to apply this approach to simulate the OCDT signal and to estimate the accuracy of the velocity profile reconstruction.

2. The simulated setup

The simulated setup (Fig. 1) is the OCDT system based on a Michelson interferometer with a superluminescent diode

A.V. Bykov, M.Yu. Kirillin, A.V. Priezzhev Deparment of Physics and International Teaching and Research Laser Center, M.V. Lomonosov Moscow State University, Vorob'evy gory, 119992 Moscow, Russia; e-mail: avp2@mail.ru; kirillin@rambler.ru

Received 18 January 2005
Kvantovaya Elektronika **35** (2) 135 – 139 (2005)
Translated by M.N. Sapozhnikov

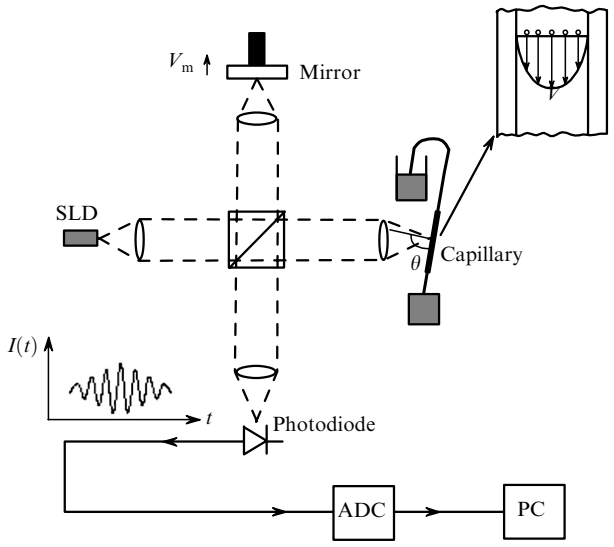

Figure 1. Simulated setup and the object under study. The signal from a single scatterer is shown.

emitting at 633 or 822 nm and having the coherence length $l_{coh} = 15$ μm. The velocity of a scanning mirror in the reference arm of the interferometer is $V_m = 12$ mm s^{-1}. We studied the laminar flow of a 1-mm thick plane intralipid layer between two plane–parallel 0.25-mm thick glass plates in the air. The intralipid is a suspension of lipid particles of different sizes and concentrations and is often used in experiments for simulating biological tissues [12, 13]. The volume concentration of intralipid C was varied from 0.7 % to 1.5 %, which corresponds to the change in the scattering coefficient of the suspension from 0.25 to 5.25 mm^{-1} at 633 nm and from 0.2 to 4 mm^{-1} at 822 nm. The absorption of light by intralipid is assumed negligible. The refractive indices of the intralipid and glass are 1.36 and 1.50, respectively. The velocity profile in the medium is assumed parabolic, with the maximum velocity $V_{max} = 256$ mm s^{-1} at the capillary centre. The angle between the initial direction of the incident beam and the direction of the flow velocity vector was taken to be 88°. These parameters correspond to real experimental conditions described in [14]. Photons scattered strictly backward within the angular aperture of 6° are assumed detected. The angle between this direction and the normal to the surface of the medium under study was 2°,

3. Algorithm for signal simulation

Upon the dynamic interference of light waves incident on a photodetector from the object and reference arms, the output electric signal of the photodetector appears in the form of amplitude-modulated pulses. Each of the pulses is the signal from a certain optical inhomogeneity (for example, from the interface of media with different refractive indices, from a scattering particle, etc.). The modulation amplitude and frequency of such a pulse are determined by the difference of the refractive indices of the media and the velocity of the scanning mirror in the reference arm, respectively, while its envelope is determined by the coherence function of the light source. The envelope characterises the spatial localisation of the inhomogeneity. Therefore, the smaller is the coherence length l_{coh}, the shorter is the pulse and the higher is the resolution of the OCDT system.

The Monte Carlo simulation of the propagation of light in highly scattering media is based on multiple calculations of a random trajectory of a single photon in a medium and the subsequent statistical generalisation of the obtained data [15]. The main input parameters of the medium used in simulations are the scattering coefficient μ_s, the absorption coefficient μ_a, the anisotropy factor g (the average cosine of the scattering angle), and the phase function of a scatterer. The model parameters were calculated from the available data for the 10 % intralipid [12, 13] assuming that μ_s depends linearly on the concentration, while the phase function and the anisotropy factor remain constant at any intralipid concentrations. Such an assumption is valid because we considered in this paper only comparatively low volume concentrations of intralipid C. Absorption at such concentrations is very weak and can be neglected, i.e., $\mu_a = 0$. The values of parameters used in simulations are presented in Table 1.

Table 1. Optical parameters of the intralipid at its different concentrations.

C (%)	$\lambda = 633$ (822) nm	
	μ_s/mm^{-1}	g
0.07	0.25 (0.2)	0.83 (0.7)
0.37	1.30 (1)	0.83 (0.7)
0.75	2.60 (2)	0.83 (0.7)
1.50	5.25 (4)	0.83 (0.7)

We adapted the algorithm and our program of the Monte Carlo simulation of light propagation in highly scattering media, described earlier in [10], for calculating the OCDT signal from a moving intralipid suspension taking into account the optical mixing of photons that have come from the reference and object arms, which corresponds in the wave representation to the dynamic interference of the reference and object waves. The simulation involves two stages. First we calculated the trajectories of single photons and their Doppler frequency shifts by the standard Monte Carlo algorithm with the use of the Heyney–Greenstein phase function [10]. Then, the time dependence of the OCDT signal was constructed in the process of scanning over the depth taking into account all the detected photons and the conditions of optical mixing on the photodetector, as well as the coherence function of the source. For this purpose, the entire scanning time interval was divided into 100 thousand intervals, and the total number of photons incident on the detector was calculated in each of the intervals and their average Doppler frequency was determined. Then, taking the corpuscular-wave dualism into account, in accordance with the expression [2]

$$I_{int} = \frac{1}{2} E_r E_s \cos\left(\frac{2\pi}{\lambda}\Delta l\right) \quad (1)$$

for the interference term (where E_r and E_s are the amplitudes of the waves scattered in the reference and object arms, respectively, and Δl is the optical path difference), we calculated the interference signal, taking the Doppler shift into account, from the expression

$$I = \sqrt{N_r N_x}\cos\left[\left(\frac{2\pi}{\lambda}+\frac{2\pi\Delta f}{V_m}\right)\Delta l\right]\exp\left[-\left(\frac{\Delta l}{l_{coh}}\right)^2\right]. \qquad (2)$$

Here, N_r and N_s are the numbers of photons incident on the detector from the reference and object arms, respectively, during the given time interval with the given optical path difference; Δf is the average value of the Doppler shifts for photons that came from the object arm during the same time interval. The coherence function was described by a Gaussian, as demonstrated by the exponential in (2).

We assumed in calculations that the total distribution of photons (over mean free paths, Doppler shifts, etc.) in the subsequent time interval is the same as in the previous one, which corresponds to a stable continuous radiation of the source. Photons arriving during one interval were assumed simultaneous, and their contribution to the signal was calculated from expression (2). The calculation statistics was 100 million photons per realisation (A scan) of the model signal.

4. Results and discussion

We calculated model OCDT signals from a plane layer of the intralipid flow for different suspension concentrations at two wavelengths. Figure 2 shows two typical time dependences of the signal obtained by scanning over the flow depth at a wavelength of 822 nm. In both cases, only a part of the signal corresponding to scattering from the medium between the inner walls of the capillary is shown, i.e., the part of the signal containing information on the velocity distribution in the flow. Signals corresponding to reflection from interfaces between the medium and the walls of glass plates confining the flow are not shown.

One can see from Fig. 2b that the signal strongly decays with time because of strong scattering at high intralipid concentrations, which corresponds to a decrease in the intensity of a signal arriving from greater depths. This results in a decrease in the number of photons carrying information from large depths and in an increase in the error in the determining velocity at large depths. The distribution of flow velocities over the depth (velocity profile) was constructed by dividing the temporal realisation

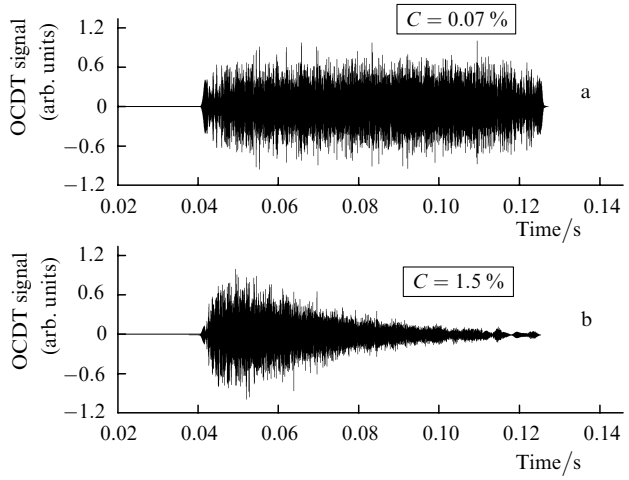

Figure 2. Typical OCDT signals for $\lambda = 822$ nm from the intralipid flow with different volume concentrations C in a plane layer, which are the time dependences of the interference signal intensity on the photodetector.

of the signal into 50 successive sections and averaging Doppler shifts and, hence, velocities in each of these sections. Then, the Doppler frequency was determined for each of the sections with the help of the fast Fourier transform, and the flow velocity corresponding to this frequency was found from the expression

$$V_i = \frac{(f_d^i - f_0)\lambda}{2n\cos\theta}, \qquad (3)$$

where f_d^i is the average Doppler frequency of the ith section; f_0 is the Doppler frequency caused by reflection of radiation from the moving reference mirror; n is the refractive index of the medium; and θ is the angle between the incident radiation and the flow velocity vector.

The velocity profiles obtained at different intralipid concentrations are shown in Fig. 3. One can see that for both wavelengths the deviations of the reconstructed profile from the given one increase with increasing the intralipid concentration. This occurs because the number of doubly and multiply scattered photons incident on the detector increases with the concentration, resulting in strong variations in the Doppler frequency shifts of these photons, thereby distorting the reconstructed velocity profile. This effect is especially distinct in the measurement of velocities at depths $\sim$1 mm and greater, information on these velocities being carried in most cases by multiply scattered photons.

As the intralipid concentration was increased, the maximum of the reconstructed velocity profile shifted with respect to the given profile up to 6 % for $\lambda = 822$ nm and up to 9 % for $\lambda = 633$ nm at $C = 1.5$ % (Fig. 4). This is caused by the increased contribution of multiply scattered photons, which propagate over a greater distance on average than singly scattered photons arriving from the same depth. Therefore, the former photons contribute to the signal at later instants, which results in the velocity profile broadening and shift compared to the given profile. For each concentration, the shift of the profile maximum for the probe wavelength of 633 nm is greater than for 822 nm. This is explained by the wavelength dependence of the scattering properties of the intralipid, for which the scattering coefficient at 633 nm is higher than that at 822 nm (Table 1).

Because the scattering order of photons contributing to the signal substantially affects the parameters of velocity profiles reconstructed from the signal, we analysed the contributions from photons of different scattering orders to the OCDT signal. We found out that for the intralipid concentration $C = 0.07$ %, the contribution from singly scattered photons to the signal for both wavelengths was 99 % and the profile distortion was insignificant. For $C = 1.5$ %, the contribution from singly scattered photons is 48% (822 nm) and 34 % (633 nm), so that multiply scattered photons introduce significant distortions to the reconstructed profiles. Doubly scattered photons at $C = 0.07$ % amount to 1% of the number of all the detected photons at both wavelengths, whereas at $C = 1.5$ % their contribution is 30 % and 23 % for wavelengths 822 and 633 nm, respectively.

Figure 5 shows the scattering-order distributions of photons contributing to the OCDT signal for different wavelengths and different intralipid concentrations. One can see that as the intralipid concentration increases, the

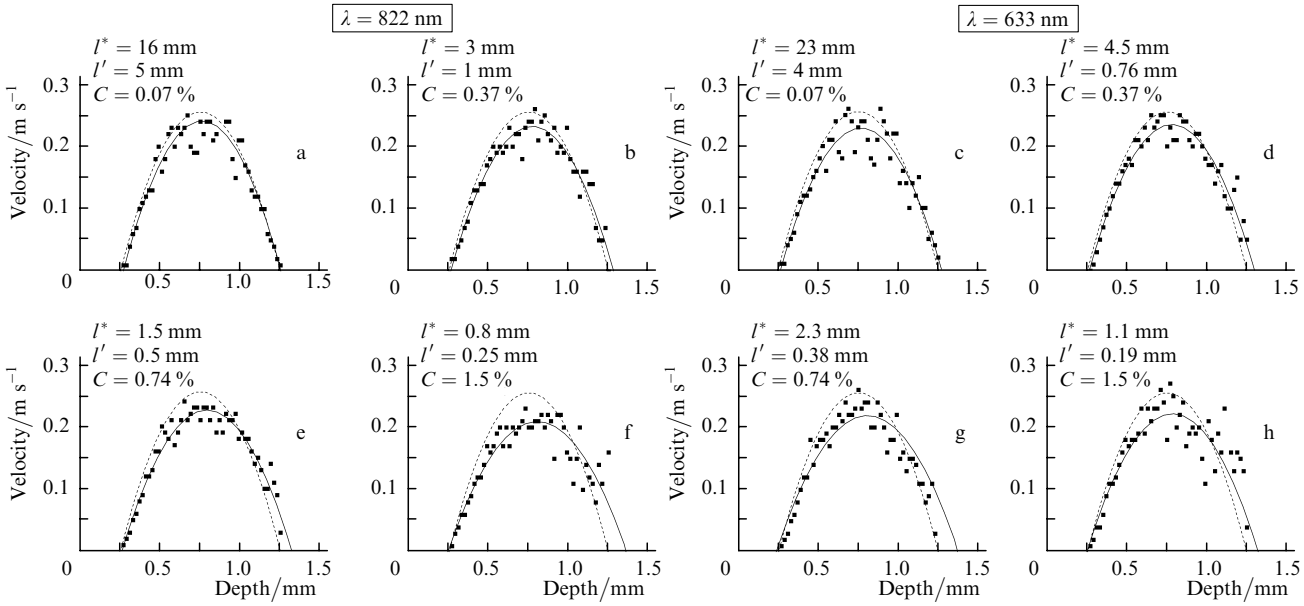

Figure 3. Comparison of the velocity profiles at different wavelengths λ, volume intralipid concentrations C, and different transport lengths l^* and mean free paths l' of photons in the medium. The dashed curve is Poiseuille's profile; the points show the profile reconstructed from the model OCDT signal; the solid curve is the parabolic approximation of the reconstructed velocity profile.

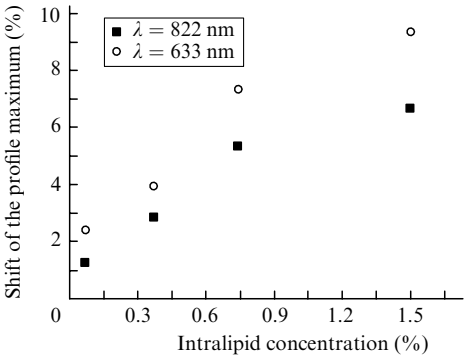

Figure 4. Dependences of the shift of the maximum of the reconstructed profile on the intralipid concentration for two wavelengths.

role of higher-order scattering increases for both wavelengths, and contributions from greater scattering orders appear, which were absent at lower concentrations. For example, at first (Fig. 5a) only singly or doubly scattered photons contribute to the signal, while then (Fig. 5b) the contribution from doubly scattered photons increases and triply scattered photons appear. Simultaneously, the contribution of singly scattered photons decreases. For a wavelength of 633 nm, also new scattering orders appear with increasing the concentration.

Because singly scattered photons play a very important role, it is necessary to analyse their contribution to the OCDT signal. The dependences of the contribution from singly scattered photons to the OCDT signal on the intralipid concentration for both wavelengths are shown in Fig. 6. For the concentrations considered here, singly scattered photons contribute no less than 30%; however, their contribution decreases with increasing intralipid concentration, resulting in the distortion of the reconstructed profile.

We also estimated the relative error of simulations as the ratio of the root-mean-square deviation of the calculated

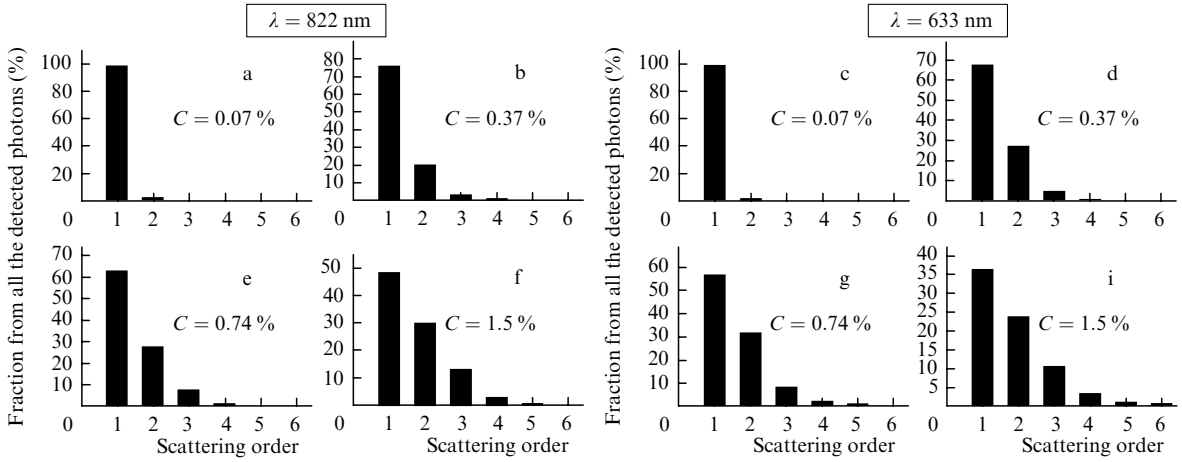

Figure 5. Contributions of photons of different scattering orders to the OCDT signal for wavelengths 822 and 633 nm at different intralipid concentrations.

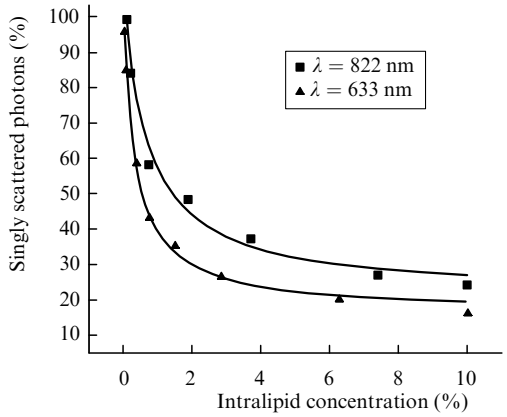

Figure 6. Dependences of the percent contribution of singly scattered photons to the OCDT signal on the intralipid concentration for two wavelengths.

quantity, determined for five realisations of the same signal, to its average value. For example, for the concentration $C = 0.37\,\%$ at 822 nm, the relative error of the flow velocity calculation is 20 % at the near wall of the capillary, 5 % in the capillary centre, and 40 % at its rear wall. A greater relative error of flow velocity measurements near capillary walls compared to that in the flow centre is explained by the fact that the relative error tends to infinity when the quantity being measured tends to zero. A greater error of flow velocity measurement near the rear wall of the capillary compared to that at the near wall is explained by a smaller number of photons arriving from the distant wall.

5. Conclusions

Our calculations have shown that the detection of multiply scattered photons at high concentrations of scatterers in a flow distorts the reconstructed velocity profile and causes the shift of its maximum. However, at the concentrations lower than ~0.4 %, at which single scattering dominates in the detected signal, the reconstructed and given Poiseuille's profiles are in good agreement within 3 %. Our simulations have shown that at comparatively low intralipid concentrations, OCDT can be used for reconstructing the velocity profile of the intralipid flow at depths up to 1 mm. At higher intralipid concentrations, the reconstructed profiles are distorted and are elongated in the direction of the rear boundary of the flow. However, in these cases, the OCDT system being simulated can be used for velocity measurements at smaller depths. Note that the results obtained in the paper depend quantitatively on the receiving aperture and focusing of the probe beam, which were assumed fixed in simulations. However, the qualitative conclusions are independent of these parameters.

Acknowledgements. This work was supported by the Leading Scientific Schools Grant No. 2071.2003.4.

References

1. Zimnyakov D.A., Tuchin V.V. *Kvantovaya Elektron.*, **32**, 849 (2002) [*Quantum Electron.*, **32**, 849 (2002)].
2. Milner T.E. et al., in *Handbook of Optical Coherence Tomography*. Ed. by B.E. Bouma, G.J. Tearney (New York: Marcel Dekker, 2002) p. 203.
3. Chen Z., Zhao Y., Srinivas S.M., Nelson J.S., Prakash N., Frostig R.D. *IEEE J. Selected Top. Quantum Electron.*, **5** (4), 1134 (1999).
4. Proskurin S.G., Yonghong He, Wang R.K. *Phys. Med. Biol.*, **49**, 1265 (2004).
5. Lindmoy T., Smithies D.J., Chen Z., Nelson J.S., Milner T.E. *Phys. Med. Biol.*, **43**, 3045 (1998).
6. Kolinko V.G., deMul F.F.M., Greve J., Priezzhev A.V. *Med. Biol. Eng. Comput.*, **35**, 287 (1997).
7. Tycho A., Jorgensen T.M., Yura H.T., Andersen P.E. *Appl. Opt.*, **41**, 6676 (2002).
8. Lopatin V.V., Priezzhev A.V., Fedoseev V.V. *Biomed. Radioelektron.*, **7**, 29 (2000).
9. Wang R.K. *Phys. Med. Biol.*, **47**, 2281 (2002).
10. Kirillin M.Yu., Priezzhev A.V. *Kvantovaya Elektron.*, **32**, 883 (2002) [*Quantum Electron.*, **32**, 883 (2002)].
11. Priezzhev A.V., Fedoseev V.V., Kudinov D.A. *Proc. SPIE Int. Soc. Opt. Eng.*, **3726**, 567 (1999).
12. Flock S.T., Jacques S.L., Wilson B.C., Star W.M., van Gemert M.J.C. *Lasers in Surgery and Medicine*, **12**, 510 (1992).
13. Van Staveren H.G., Moes C.J.M, van Marle J., Prahl S.A., van Gemert M.J.C. *Appl. Opt.*, **30**, 4507 (1991).
14. Hast J., Prykari T., Alarousu E., Myllyla R., Priezzhev A.V. *Proc. SPIE Int. Soc. Opt. Eng.*, **4965**, 66 (2003).
15. Kandidov V.P. *Usp. Fiz. Nauk.*, **166**, 1309 (1996).